PHYSICAL REVIEW B **82**, 085302 (2010)

Origin of the bias stress instability in single-crystal organic field-effect transistors

B. Lee,[1] A. Wan,[2] D. Mastrogiovanni,[2] J. E. Anthony,[3] E. Garfunkel,[2,4] and V. Podzorov[1,4,*]
[1]*Department of Physics, Rutgers University, Piscataway, New Jersey 08854, USA*
[2]*Department of Chemistry, Rutgers University, Piscataway, New Jersey 08854, USA*
[3]*Department of Chemistry, University of Kentucky, Lexington, Kentucky 40506, USA*
[4]*Institute for Advanced Materials, Devices and Nanotechnology, Rutgers University, Piscataway, New Jersey 08854, USA*
(Received 23 May 2010; published 3 August 2010)

We report a systematic study of the bias stress effect at semiconductor-dielectric interfaces using single-crystal organic field-effect transistors as a test bed. A combination of electrical transport and ultraviolet photoelectron spectroscopy suggests that this instability is due to a ground-state (i.e., occurring in the dark) charge transfer of holes from the accumulation channel of the semiconductor to localized states of a disordered insulator. The proposed model is not semiconductor specific and therefore provides a general analytical description of this instability in a variety of organic and inorganic band semiconductors interfaced with amorphous insulators.

DOI: 10.1103/PhysRevB.82.085302 PACS number(s): 73.20.At, 73.20.Hb, 73.25.+i

The bias stress effect is a longstanding problem in organic and inorganic semiconductor field-effect transistors (FETs) (see, e.g., Ref. 1). Investigation of this phenomenon is not only of practical importance but may also offer insights into fundamentals of energetic structure of semiconductor-dielectric interfaces.[2] The effect presents itself as a continuous decrease of the current in the channel (or a shift of the threshold voltage) observed under accumulation conditions. Although bias stress effect has been studied in amorphous Si and lately in organic thin-film FETs, disorder present in these materials (e.g., ubiquitous grain boundaries[3]) leads to a significant charge scattering, trapping, and other nonintrinsic contributions to the transport properties. Several of the proposed mechanisms of the effect (recently reviewed in Ref. 1) are indeed related to extrinsic phenomena, such as, e.g., (a) trapping of holes in the semiconductor's channel, (b) injection of electrons from the gate electrode into the dielectric, (c) ionic conduction in the dielectric, and (d) modification of contacts under the gate bias. While all these effects are important for applications, the question still remains whether there is an intrinsic mechanism of the bias stress instability at well-defined semiconductor-dielectric interfaces without any involvement of ambient environmental factors or trapping in the semiconducting channel. Recently developed highly ordered single-crystal organic field-effect transistors (OFETs) allow us to address this problem.[4–6] The conclusions drawn from our experiment are not specific only to organic semiconductors and can be applied to any band (semi)conducting material, such as, for example, Si, carbon nanotubes (CNTs), or graphene, interfaced with an amorphous dielectric (SiO_2, high-k oxides or nonconjugated polymers).

In this study, we have investigated the bias stress effect in OFETs based on single crystals of several organic semiconductors: rubrene,[7] tetracene,[8] and 6,13-bis[triisopropylsilylethynyl] (TIPS) pentacene,[9] that have been interfaced with a nonconjugated polymer, parylene, previously used as an insulator in high-performance OFETs.[4] Investigations of this type of semiconductor-insulator interfaces are critically important because practical organic electronic devices will ultimately rely on inexpensive plastic insulators rather than expensive oxides. Rubrene and tetracene single crystals have been grown by physical vapor transport (see, e.g., Ref. 4). TIPS-pentacene single crystals have been prepared by crystallization from solution and annealed in a stream of forming gas (100 cc/min) at 120 °C for 4 h before OFET fabrication. Fabrication of optimized devices is described elsewhere[4,7]). Field-effect mobilities, μ, were obtained from the linear transconductance curves, $I_{SD}(V_G)$—the dependence of the source-drain current, I_{SD}, on the gate voltage, V_G, at a fixed source-drain voltage, V_{SD}. We have verified that contact resistance effects in our OFETs were negligible before and after gate stressing.

Figure 1 shows the typical bias stress characteristics of our OFETs, i.e., $I_{SD}(t)$ measured in the dark at fixed V_G and V_{SD}. We define the magnitude of the bias stress as $\Delta I/I_0 = [I_0 - I(t)]/I_0$, where I_0 is the initial source-drain current established right after the transistor is on. In rubrene OFETs, the dark bias stress effect is very small; the current decreases by only 5–7 % after a continuous stressing for 6 h at $V_G = -80$ V while in TIPS pentacene and tetracene devices it is typically about 30% and 45%, respectively. Transconductance measurements before and after a prolonged stressing indicate that the slope of $I_{SD}(V_G)$ does not change in any of the studied systems, i.e., the bias stress effect is solely due to a shift of the threshold voltage without changes in μ (inset in the top panel of Fig. 1) and hence measuring $I_{SD}(t)$ is analogous to measuring the threshold voltage shift. In addition, the preserved linear mobility in these two-probe OFETs suggests that the contact resistance is not much affected by the stress.[7] It is also interesting that the threshold voltage shift can be partially recovered by a prolonged application of a positive V_G. However, complete recovery in these p-type OFETs cannot be achieved because at $V_g > 0$ there is no accumulation channel and hence the electric field at the interface is much weaker than the field at equivalent $V_g < 0$.

Two striking features of the bias stress instability can be seen at Fig. 1. First, the rate and the magnitude of the effect strongly depend on the type of organic semiconductor, rather than on the typical charge-carrier mobility in each system. For instance, although TIPS-pentacene OFETs have $\mu \sim 0.05 \pm 0.01$ cm^2 V^{-1} s^{-1}, which is not unusual for solution-grown single crystals with rough facets,[9,10] the bias

 ©2010 The American Physical Society

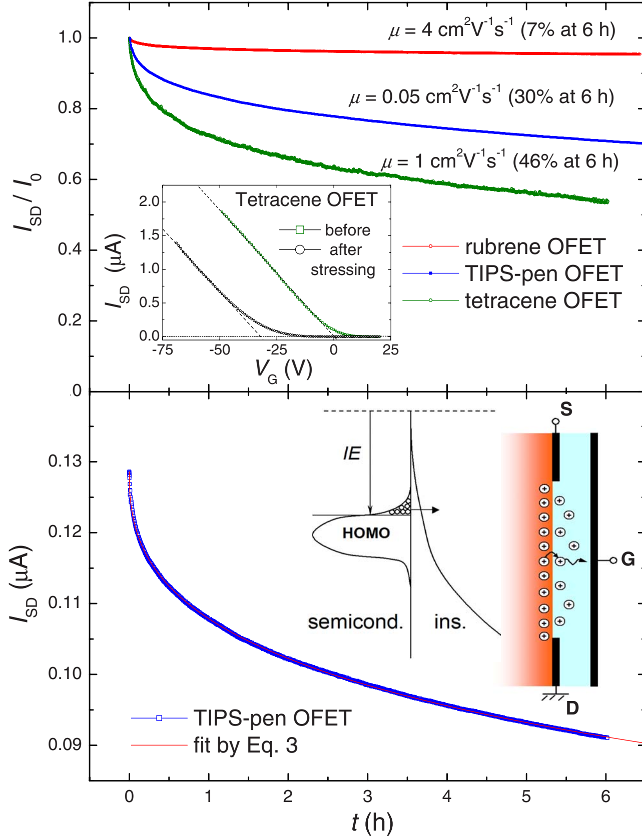

FIG. 1. (Color online). Top: normalized bias stress curves, $I_{SD}(t)/I_0$, of several single-crystal OFETs ($V_G=-80$ V, $V_{SD}=25$ V, $C_i=2.35$ nF/cm^2). The typical linear field-effect mobilities, μ, and the bias stress values at 6 h of continuous stressing are indicated for each system. The inset shows that the slope of $I_{SD}(V_G)$ does not change after stressing for 6 h. Bottom: the bias stress curve of a TIPS-pentacene OFET fitted with a stretched hyperbola [Eq. (3)]. Similar fits are obtained for the other systems. The inset shows an energy model of the semiconductor-insulator interface: the hole transfer rate depends on the overlap between the semiconductor's HOMO and the exponential tail of localized states of the insulator. The cartoon schematically depicts the transfer and drift of holes in the insulator.

stress effect in these devices is typically smaller than that in tetracene OFETs with $\mu \approx 1$ cm^2 V^{-1} s^{-1} (Fig. 1). This trend has been verified in multiple devices measured in our laboratory over the course of several years. Second, all the devices exhibit the same characteristic type of the bias stress curve independently on the overall magnitude of the effect: an initial fast decay of I_{SD} and a subsequent much slower relaxation that can continue for hours or days, as long as V_G is applied.

In the prior studies, such distinct shape has been empirically fitted with a stretched exponent, adopted from amorphous Si transistor research, where the bias stress is believed to be due to dispersive diffusion of hydrogen in α-Si.[1,11] It is important to note that although a stretched exponential decay provides a satisfactory fit to most of the OFET data,[1] a detailed microscopic model explaining such behavior in organic semiconductors is lacking. It is especially difficult to justify such model in the case of highly ordered molecular crystals, where the charge transport cannot be described as a dispersive hopping in exponentially distributed trap states, necessary to obtain a stretched exponential dependence.[1]

We argue that the leading mechanism of the bias stress instability in our OFETs is a ground-state *hole transfer* from the field-induced accumulation channel of the organic semiconductor to localized states of the adjacent insulator (sketch at Fig. 1). The transferred holes, located between the accumulation channel and the gate, are screening the gate electric field, so it's effective value in the channel becomes $E_G \equiv en_{ch}(t)/(\varepsilon\varepsilon_0)=(V_G/d)-en(t)/(\varepsilon\varepsilon_0)$, where e is the elementary charge, ε and ε_0 are the dielectric permittivities of the insulator and free space, respectively, $n(t)$ is an areal (i.e., two-dimensional) density of the transferred holes, d is the insulator thickness, $n_{ch}(t)$ is the density of mobile holes in the OFET channel that becomes smaller as the result of screening, leading to a decreasing source-drain current: $I_{SD}(t)=(W/L)\cdot V_{SD}\cdot \mu e \cdot n_{ch}(t)$. The density of transferred charge $n(t)$ is related to $n_{ch}(t)$ as $n(t)+n_{ch}(t)=n_0$, where the constant $n_0 \equiv n_{ch}(t=0)=\varepsilon\varepsilon_0 V_G/(ed)$ is the initial density of holes in the channel.

The charge-transfer rate, dn/dt, should be proportional to the density of holes available in the accumulation channel, n_{ch}, and a three-dimensional density of states, δ_0, in the exponentially distributed tail states of the disordered insulator at an energy matching the semiconductor's highest occupied molecular orbital (HOMO) edge, where holes are accumulated in OFETs (Fig. 1). The magnitude δ_0 depends on the relative position of ionization energies (IEs) of the semiconductor and the insulator, as well as on the extent of the tail states of the latter. In addition, since the process of filling δ_0 states by interfacial charge transfer is fast, the rate of the bias stress effect will be mainly limited by the secondary process—a slow *diffusion* or *drift* of the transferred holes away from the interface (toward the gate), as the result of which some of the insulator's states near to the interface become empty and available again for further hole transfer. Therefore, dn/dt must be proportional to the sum of diffusion and drift fluxes of holes in parylene, $j_{diff} \approx D_{ins}\cdot \delta_0/\lambda_0$, and $j_{drift}=\delta_0\cdot \nu_{drift}=\delta_0\cdot \mu_{ins}\cdot E_G=\delta_0\cdot \mu_{ins}\cdot en_{ch}/(\varepsilon\varepsilon_0)$, where D_{ins} is a diffusivity of holes in the insulator, λ_0 is a characteristic width of the spatial distribution of holes in the insulator near the interface, $\nu_{drift}\equiv \mu_{ins}\cdot E_G$ is a drift velocity of holes with hopping mobility μ_{ins} in the insulator near the interface. μ_{ins} in nonconjugated insulators is extremely small and to the first approximation does not show a Poole-Frenkel dependence because of (a) relatively small E_G used in our study and (b) undoped and nonpolar nature of parylene without spatial correlations of energetic disorder.[12] Hence, the charge-transfer rate can be expressed as $dn/dt \equiv -dn_{ch}/dt = \chi_0\cdot n_{ch}\cdot (j_{diff}+j_{drift})$ or

$$dn_{ch}/dt = -\chi_0 n_{ch}(D_{ins}\delta_0/\lambda_0 + \delta_0\mu_{ins}E_G), \qquad (1)$$

where χ_0 is a cross section of the charge-transfer process in square centimeters.

Dispersive transport in virtually all disordered systems with an exponential distribution of band tails universally exhibits a power-law time dependence of diffusivity and mobility, $D_{ins}=D_0\cdot (t/\tau_{ins})^{\beta-1}$ and $\mu_{ins}=\mu_0\cdot (t/\tau_{ins})^{\beta-1}$, where τ_{ins}

is the characteristic trapping time in the insulator ($1/\tau_{ins}$ is the hopping rate) at the transport energy level (not to be confused with HOMO edge), and $\beta \equiv T/T_0 < 1$ is a dispersion exponent related to the characteristic width of the band tail of the insulator.[1,13,14] Hence, we can rewrite Eq. (1) as

$$dn_{ch}/dt = -\chi_0 \cdot (t/\tau_{ins})^{\beta-1} \cdot [D_0(\delta_0/\lambda_0) \cdot n_{ch} + \delta_0\mu_0 e/(\varepsilon\varepsilon_0) \cdot n_{ch}^2]. \quad (2)$$

Note that if the charge motion in the insulator is dominated by diffusion ($j_{diff} \gg j_{drift}$), the rate of the bias stress effect will be proportional to n_{ch} or V_G, and the solution of Eq. (2) will be a stretched exponent, $n_{ch}(t) = n_0 \exp[-(t/\tau)^\beta]$, where τ is a renormalized V_G-independent time constant $\tau = \tau_{ins} \cdot [\lambda_0\beta/(\chi_0 D_0 \delta_0 \tau_{ins})]^{1/\beta}$. However, if the process is dominated by drift ($j_{diff} \ll j_{drift}$), dn/dt will be proportional to n_{ch}^2 or V_G^2 and the analytical solution of Eq. (2) for the source-drain current $I_{SD} = (W/L)V_{SD}\mu e \cdot n_{ch}$ is a stretched hyperbola

$$I_{SD}(t) = \frac{I_0}{1 + (t/\tau)^\beta}, \quad \tau = \tau_{ins} \cdot \left(\frac{\beta d}{V_G \chi_0 \mu_0 \delta_0 \tau_{ins}}\right)^{1/\beta}, \quad (3)$$

where $I_0 \equiv I_{SD}(t=0)$ is the initial current in the channel and τ is a renormalized V_G-dependent time constant. In both cases, the time constant τ increases as $(1/\delta_0)^{1/\beta}$ for interfaces with a smaller energetic overlap δ_0, because $\beta > 0$.

In our experimental situation, the hole motion in the insulator is drift limited. Indeed, we have estimated that the ratio $j_{drift}/j_{diff} = (\lambda_0\mu_0 V_G)/(D_0 d) = (eV_G/k_B T) \cdot (\lambda_0/d) \sim 10-30 \gg 1$, with $D_0 = k_B T \mu_0/e$ (k_B is the Boltzmann constant), and $\lambda_0 \sim 3-10$ nm—a reasonable lower limit of the distance at which holes are injected into the parylene. Moreover, we have confirmed the drift-limited regime experimentally by measuring the actual dependence of the bias stress rate, dI_{SD}/dt, on V_G in a number of nominally identical rubrene transistors (Fig. 2). The inset in Fig. 2 shows that the bias stress effect is indeed greater at a higher V_G, and the rate follows a V_G^2 dependence (the lower panel), as expected from Eq. (2) in this regime. In addition, fitting the four curves in the inset with a stretched hyperbola [Eq. (3)] yields a V_G-dependent τ and a value of $\beta = 0.3 \pm 0.05$. According to Eq. (3), τ should be proportional to $(1/V_G)^{1/\beta}$. Plotting $\ln(\tau)$ vs $\ln(1/V_G)$ for this set of devices indeed results in a linear dependence with a slope consistent with $\beta \sim 0.3$ (the upper panel of Fig. 2).

A stretched hyperbola [Eq. (3)] provides a perfect fit to all of the studied systems (for simplicity, the lower panel of Fig. 1 shows only the fit for TIPS-pentacene OFET). It is worth noting that τ and β obtained by fitting these systems are consistent with the underlying physics of the effect. Indeed, τ decreases in the order: rubrene (49.5×10^6 s), TIPS pentacene (0.177×10^6 s) and tetracene (0.031×10^6 s), consistent with the bias stress rate increasing in this order and implying that δ_0 is also increasing in the same order [we confirm this trend below by ultraviolet photoemission spectroscopy (UPS)]. However, the exponent β in this set is found to be almost constant: $\beta = 0.37 \pm 0.05$.

According to our model, organic transistors with a greater energetic overlap between HOMO and localized states of the insulator should exhibit a stronger bias stress effect (Fig. 1).

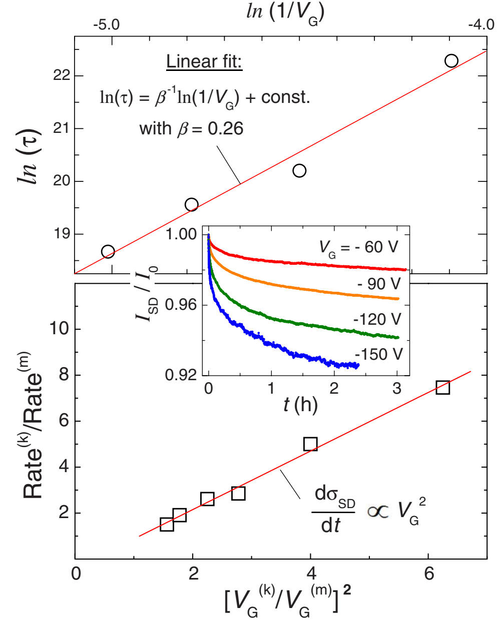

FIG. 2. (Color online). Bias stress effect in rubrene OFETs measured at different V_G (inset). Top: V_G dependence of the time constant τ, obtained for the four curves by stretched hyperbola fits [Eq. (3)]. Bottom: ratio of the bias stress rates measured at different V_G and plotted as a function of V_G ratios squared. Red line is a linear fit.

In order to test this idea, we have performed UPS studies of ionization energies (IEs) of the organic crystals and the insulator used in this study (Fig. 3) (details of UPS technique can be found elsewhere[15]). IE refers to position of the HOMO edge with respect to the vacuum level (i.e., it is an energetic position of holes in the accumulation channel in *p*-type OFETs). The IEs of rubrene, TIPS pentacene, tet-

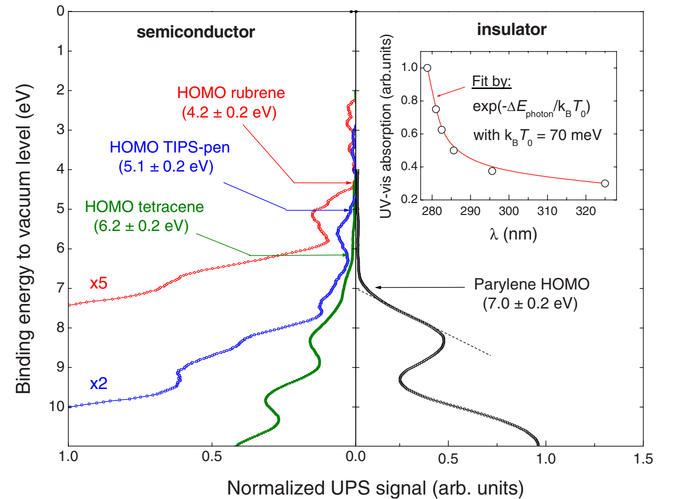

FIG. 3. (Color online) Left: UPS spectra of crystalline rubrene (red), TIPS pentacene (blue), and tetracene (green). Photoemission onsets (i.e., HOMO edges or IEs) referenced to the vacuum level are shown with the arrows. Right: UPS spectrum of an ultrathin (10 ± 2 nm) parylene *N* on gold. The inset is a UV-visible optical-absorption spectrum of parylene *N*, showing a ~1.5-eV-wide tail of states below the 280 nm absorption edge.

racene, and parylene are 4.2 ± 0.2 eV, 5.1 ± 0.2 eV, 6.2 ± 0.2 eV, and 7.0 ± 0.2 eV, respectively. Despite a considerable difference between the HOMOs of the organic semiconductors and parylene, the exponential tail states of the latter (seen above 7 eV in Fig. 3) allow for a small charge transfer. A better evidence of the extended in-gap tail states of parylene is provided by the UV-visible absorption of this material (inset in Fig. 3). As expected, the absorption edge (280 nm) considerably tails into the band gap. Fitting this tail with an exponential distribution yields $k_BT_0\approx 70$ meV, in a good agreement with a room-temperature value of $\beta=T/T_0\sim 0.37$. The relative positions of the semiconductor's and the insulator's HOMOs determined from our UPS are consistent with the observed trend for the rate of the bias stress effect to increase for semiconductors with a "deeper" HOMO.

It is worth noting that vacuum-gap OFETs exhibit a negligible bias stress, provided that there are no polar molecules in the residual gas in the gap. However, these devices do show a bias stress effect of a different kind that occurs as a result of an introduction of polar molecules in a gaseous form in the gap (e.g., acetone or water vapor), resulting in the effect proportional to the dipole moment of the molecules due to the gate-induced polarization of the vapor.

Most of the extrinsic factors contributing to bias stress can be ruled out in our devices. For example, charge trapping in the accumulation channel cannot be the primary cause because there are examples of OFETs with a high trap density (low μ) that nevertheless show noticeably smaller bias stress effect than other devices with a much greater μ. The influence of water at the interface or in the dielectric can also be ruled out because it would not result in a systematic dependence of the effect on the HOMO energy. In addition, (a) we have tested that *in situ* annealing of the samples at moderate temperatures in vacuum before parylene deposition does not influence the effect and (b) we have used macroscopic grain-boundary free organic crystals encapsulated in a nonhygroscopic parylene deposited in vacuum and capped with a 50-nm-thick Ag gate. Hence, postfabrication water permeation would be highly unlikely. Finally, an injection of electrons from the metal gate into the insulator in our OFETs is excluded because of the outstanding insulating properties of parylene revealed in *I-V* measurements of Ag/parylene/Ag sandwich structures, showing a typical insulating behavior with a very large resistivity, $\rho > 100$ GΩ for up to ± 200 V.

To conclude, we have systematically studied the (dark) bias stress instability in OFETs based on rubrene, tetracene, and TIPS pentacene interfaced with an amorphous polymer insulator. A combination of charge transport and UPS measurements suggests that the effect is due to a transfer of holes from the accumulation channel of the semiconductor to localized states of the insulator. The effect is smaller in systems with a greater energetic mismatch between the HOMO edges of the semiconductor and the insulator. Our model only relies on the concepts of semiconductor's ionization energy and exponential band tails of disordered insulators and hence it could be used to understand instabilities in a wider range of semiconductor devices, including organic, inorganic, CNT, and graphene FETs.

This work has been financially supported by NSF under Grants No. ECCS-0822036 and ARRA CAREER No. DMR-0843985 and Industrial Technology Research Grant Program 09E51007d (NEDO).

---

*Corresponding author; podzorov@physics.rutgers.edu

[1] H. Sirringhaus, Adv. Mater. **21**, 3859 (2009).
[2] D. Cahen, A. Kahn, and E. Umbach, Mater. Today, **8**, 32 (2005).
[3] K. Puntambekar, J. Dong, G. Haugstad, and C. Daniel Frisbie, Adv. Funct. Mater. **16**, 879 (2006).
[4] R. W. I. de Boer, M. E. Gershenson, A. F. Morpurgo, and V. Podzorov, Phys. Status Solidi **201**, 1302 (2004).
[5] J. Takeya, T. Nishikawa, T. Takenobu, S. Kobayashi, Y. Iwasa, T. Mitani, C. Goldmann, C. Krellner, and B. Batlogg, Appl. Phys. Lett. **85**, 5078 (2004).
[6] A. L. Briseno, R. J. Tseng, M.-M. Ling, E. H. L. Falcao, Y. Yang, F. Wudl, and Z. Bao, Adv. Mater. **18**, 2320 (2006).
[7] V. Podzorov, S. E. Sysoev, E. Loginova, V. M. Pudalov, and M. E. Gershenson, Appl. Phys. Lett. **83**, 3504 (2003).
[8] M. F. Calhoun, C. Hsieh, and V. Podzorov, Phys. Rev. Lett. **98**, 096402 (2007).
[9] J. G. Park, R. Vasic, J. S. Brooks, and J. E. Anthony, J. Appl. Phys. **100**, 044511 (2006).
[10] S. Subramanian, S. K. Park, S. R. Parkin, V. Podzorov, T. N. Jackson, and J. E. Anthony, J. Am. Chem. Soc. **130**, 2706 (2008).
[11] W. B. Jackson, J. M. Marshall, and M. D. Moyer, Phys. Rev. B **39**, 1164 (1989).
[12] Y. N. Gartstein and E. M. Conwell, Chem. Phys. Lett. **245**, 351 (1995).
[13] D. Monroe, Phys. Rev. Lett. **54**, 146 (1985).
[14] H. Scher and E. W. Montroll, Phys. Rev. B **12**, 2455 (1975).
[15] A. Kahn, N. Koch, and W. Gao, J. Polym. Sci., Part B: Polym. Phys. **41**, 2529 (2003).